Spatially modulated instabilities for scaling solutions at finite charge density

Sera Cremonini

*DAMTP, Centre for Mathematical Sciences, University of Cambridge, Wilberforce Road,
Cambridge CB3 0WA, United Kingdom and George and Cynthia Mitchell Institute
for Fundamental Physics and Astronomy, Texas A&M University,
College Station, Texsas 77843–4242, USA*

We consider finite charge density geometries which interpolate between $AdS_2 \times \mathbb{R}^2$ in the infrared and AdS_4 in the ultraviolet, while traversing an intermediate regime of anisotropic Lifshitz scaling and hyperscaling violation. We work with Einstein-Maxwell-dilaton models and only turn on a background electric field. The spatially modulated instabilities of the near-horizon AdS_2 part of the geometry are used to argue that the scaling solutions themselves should be thought of as being unstable—in the deep infrared—to spatially modulated phases. We identify instability windows for the scaling exponents z and θ, which are refined further by requiring the solutions to satisfy the null energy condition. This analysis reinforces the idea that, for large classes of models, spatially modulated phases describe the ground state of hyperscaling violating scaling geometries.

I. INTRODUCTION

Recent years have seen growing interest in applying AdS/CFT methods to condensed matter systems whose underlying degrees of freedom are strongly coupled and notoriously difficult to explore using traditional methods. New gravitational solutions and instabilities have provided a rich playground for describing novel phases of quantum matter whose behavior is poorly understood. As an example, classes of scaling geometries which break Lorentz invariance have been used to model some of the unconventional properties observed in non-Fermi liquids and strongly correlated electron systems.

Lately the focus has shifted to probing and classifying gravitational solutions with spatial anisotropy and/or inhomogeneities, motivated by new qualitative and quantitative insights into transport in systems with broken translational invariance. A rich structure has emerged from holographic realizations of spatially modulated phases (see [1–4] for early work), which appear in condensed matter in a number of settings—nematics, smectics and charge/spin density waves being prime examples. Interestingly, some of the anisotropic ground states resulting from the breaking of translational invariance have played a key role in recent attempts to model holographically the formation of a crystal structure (see e.g. [5]). We refer the reader to [6–10] for recent constructions of the inhomogeneous geometries resulting from the back-reaction of spatially modulated perturbations.

In this paper, we are interested in the deep infrared fate of a class of (four-dimensional) solutions which exhibit anisotropic Lifshitz scaling and hyperscaling violation. As we will see shortly, they arise as exact solutions to simple Einstein-Maxwell-dilaton models [11–17]. More generally, however, they should be thought of as arising in the intermediate, "mid-infrared" region of more complicated

geometries, which typically flow in the infrared to either $AdS_2 \times \mathbb{R}^2$ (as emphasized in [18–21]) or a spacetime conformal to it. In the former case, the extensive entropy associated with the $AdS_2 \times \mathbb{R}^2$ near-horizon description raises the question of what is the nature of their true ground state.

It is by now well known that $AdS_2 \times \mathbb{R}^2$ suffers from spatially modulated instabilities in a number of constructions (see e.g. [22,23]). The presence of such unstable modes suggests that, in appropriate regions of phase space, the endpoint of scaling solutions with a "naïve" AdS_2 infrared completion should also be spatially modulated phases. This logic was advocated in [24] for anisotropic, hyperscaling violating solutions supported by a constant magnetic field. It was also corroborated by the complementary analysis of [25], which identified striped instabilities by examining the scaling geometries directly (without assuming a flow to AdS_2 in the IR), but relied crucially on the presence of an axionic term. In fact, in all of these cases, the presence of instabilities was directly tied to terms that violated time reversal (T) and parity (P) invariance. However, it emphasized recently in [26] that T and/or P violation are in fact *not* needed in order for $AdS_2 \times \mathbb{R}^2$ to become unstable to spatially modulated perturbations.

Here we revisit the analysis of [24] and apply it to scaling solutions at finite charge density, more relevant to the condensed matter context and in particular to compressible phases of matter. As in [24], we will rely on the assumption that these scaling solutions are approaching $AdS_2 \times \mathbb{R}^2$ in the infrared. Building on [26], we will identify the onset of spatially modulated instabilities for certain classes of anisotropic, hyperscaling violating solutions. Ensuring that null energy conditions are satisfied will refine the analysis further. As we will see, for large classes of models phases

with stripe order arise quite generically as the natural infrared description of these scaling solutions.

II. THE SETUP

We work with four-dimensional Einstein-Maxwell-dilaton (EMD) gravity,

$$\mathcal{L} = R - \frac{1}{2}(\partial\phi)^2 - f(\phi)F_{\mu\nu}F^{\mu\nu} - V(\phi), \tag{1}$$

with the scalar potential $V(\phi)$ and the gauge kinetic coupling $f(\phi)$ for now left entirely arbitrary. The equations of motion for this system are

$$R_{\mu\nu} = \frac{1}{2}(\partial_\mu\phi\partial_\nu\phi + Vg_{\mu\nu}) - \frac{1}{2}f(g_{\mu\nu}F^2 + 4F_{\mu\rho}F_\nu^\rho),$$

$$\nabla_\mu(fF^{\mu\nu}) = 0, \qquad \Box\phi - V' - f'F^2 = 0. \tag{2}$$

The background gauge field is taken to be purely electric, with $A_t = Q_e A(r)$ and all other components vanishing. We are interested in zero temperature geometries which interpolate between $AdS_2 \times \mathbb{R}^2$ in the deep IR and AdS_4 in the UV, while traversing *an intermediate scaling region* described by

$$ds^2 = r^{-2+\theta}(-r^{-2(z-1)}dt^2 + dr^2 + d\vec{x}^2). \tag{3}$$

In addition to the dynamical critical exponent z, the metric (3) is characterized by a hyperscaling violating exponent θ, thanks to which it is no longer scale invariant but transforms as $ds^2 \to \lambda^\theta ds^2$ under $t \to \lambda^z t$, $r \to \lambda r$, $x_i \to \lambda x_i$. The intermediate geometry is supported by a gauge field of the form $A \sim r^{\theta-z-2}dt$, and a running scalar, $\phi \sim \log r$, which breaks the exact Lifshitz symmetry of the metric; hence, it is only "Lifshitz-like."

The exponents $\{z, \theta\}$ modify the "usual" scalings of thermodynamic quantities, giving e.g. $s \sim T^{(d-\theta)/z}$ for the entropy of a $(d+1)$-dimensional field theory. The case $d - \theta = 1$ has received particular attention because it leads to logarithmic violations of the area law of entanglement entropy, $S_{\text{ent}} \sim A \log A$, a tell-tale of the presence of a Fermi surface [17,27]. More generally, z and θ should be thought of as tunable parameters—in the sense that they can be chosen by changing appropriately the gauge kinetic function and scalar potential of the model—and (3) as a useful laboratory to reproduce particular scalings of systems of interest.

The scaling geometries (3) arise as *exact solutions* to the model (1) when

$$f \sim e^{\alpha\phi} \quad \text{and} \quad V \sim e^{-\eta\phi}, \tag{4}$$

with $\{z, \theta\}$ related to the Lagrangian parameters $\{\alpha, \beta\}$ through

$$\theta = \frac{4\eta}{\alpha + \eta}, \qquad z = 1 + \frac{\theta}{2} + \frac{(4-\theta)^2}{2(2-\theta)\alpha^2}. \tag{5}$$

In turn, these can be inverted to give

$$\alpha^2 = \frac{(\theta-4)^2}{(\theta-2)(\theta-2z+2)}, \qquad \eta = \frac{\theta\alpha}{4-\theta}. \tag{6}$$

Finally, imposing the null energy conditions (NEC) [28] in the intermediate region further constrains the physically allowed values of z and θ,

$$(\theta-2)(2-2z+\theta) \geq 0,$$
$$(z-1)(2+z-\theta) \geq 0. \tag{7}$$

The deep infared. In the IR we require the scalar to settle to a constant, $\phi = \phi_0$, and demand the metric to become that of $AdS_2 \times \mathbb{R}^2$,

$$ds^2 = L^2\left(-r^2dt^2 + \frac{dr^2}{r^2} + d\vec{x}^2\right). \tag{8}$$

These requirements on the IR geometry are easy to satisfy for the class of theories described by (1), for appropriate choices[1] of the scalar potential $V(\phi)$ and gauge kinetic function $f(\phi)$, as shown in a number of examples in the literature. We refer the reader to the arguments of e.g. [18–21] and [24] for further details. We emphasize that in this paper we are not going to explicitly construct the solutions which interpolate between the UV and the IR $AdS_2 \times \mathbb{R}^2$ geometry, traversing the intermediate hyperscaling violating regime. We will work under the assumption that such flows can be easily realized.

The equations of motion resulting from requiring a constant scalar and the geometry (8) in the IR then yield the following near-horizon conditions on the gauge kinetic function and scalar potential,

$$V(\phi_0) = -\frac{1}{L^2}, \tag{9}$$

$$V'(\phi_0)f(\phi_0) = -V(\phi_0)f'(\phi_0), \tag{10}$$

$$Q_e^2 = -\frac{1}{2V(\phi_0)f(\phi_0)}. \tag{11}$$

We see from (9) and (11) that $V(\phi_0) < 0$ and $f(\phi_0) > 0$ are needed to ensure that the charge Q_e and the AdS radius L are real.

---

[1]They have to be such to allow the scalar to settle to a constant in the deep IR, while also sustaining an intermediate hyperscaling violating regime. The latter is guaranteed if V and f reduce to (4) in the intermediate portion of the geometry.

The ultraviolet. In order to operate within the standard holographic framework, in the deep ultraviolet we are interested in solutions which approach AdS$_4$ with a constant scalar $\phi = \phi_{\mathrm{UV}}$. The UV value of the scalar is then determined entirely by the condition that the effective scalar potential $V_{\mathrm{eff}} = V(\phi) + f(\phi)F^2$ admits an extremum, $\partial_\phi V_{\mathrm{eff}}(\phi_{\mathrm{UV}}) = 0$. However, we should emphasize that the structure of the instabilities and the main point of this analysis are linked to the infrared portion of the geometry and are largely insensitive to the UV. Thus, the main results of this paper will not be directly affected by the choice of other UV fixed points.

III. SPATIALLY MODULATED INSTABILITIES

The spatially modulated instabilities of electrically charged AdS$_2 \times \mathbb{R}^2$ solutions to the class of models (1) were analyzed recently in [26]. Here we build on the final results of their analysis and identify instability windows for the parameters of the theory—first by working in a small-momentum approximation and then by considering a few simple exact cases. In Sec. IV, we will apply this instability analysis to $\{z, \theta\}$ scaling solutions assumed to have an AdS$_2 \times \mathbb{R}^2$ infrared completion.

After turning on the following set of time dependent, spatially modulated linear fluctuations of the AdS$_2 \times \mathbb{R}^2$ background geometry,

$$
\begin{aligned}
\delta\phi &= e^{-i\omega t} h(r) \cos k x_1, \\
\delta g_{tt} &= L^2 r^2 e^{-i\omega t} h_{tt}(r) \cos k x_1, \\
\delta g_{x_i x_i} &= L^2 e^{-i\omega t} h_{x_i x_i}(r) \cos k x_1, \\
\delta g_{tx_1} &= L^2 e^{-i\omega t} h_{tx_1}(r) \sin k x_1, \\
\delta A_t &= -E e^{-i\omega t} a_t(r) \cos k x_1, \\
\delta A_{x_1} &= -E e^{-i\omega t} a_{x_1}(r) \sin k x_1,
\end{aligned} \tag{12}
$$

with $i = \{1, 2\}$ and working in radial gauge, one can use the remaining gauge freedom[2] to identify *three* gauge invariant combinations, $\Phi_i = h_{tt} + 2a'_t$, $\Phi_2 = g_{x_2 x_2}$ and $\Phi_3 = h$. Letting $\vec{v} = \{\Phi_1, \Phi_2, \Phi_3\}$, the fluctuation equations then take the form [26] of three mixed modes propagating on AdS$_2$,

$$
\left(\frac{\omega^2}{r^2} + r^2 \partial_r^2 + 2r\partial_r \right) \vec{v} = M^2 \vec{v}. \tag{13}
$$

The mass matrix M is given by[3]

$$
M^2 = \begin{bmatrix} 2 + 2\tau_1^2 + k^2 & -2k^2 & 2\tau_1(2 - k^2 - \tau_2 - v_2) \\ -1 & k^2 & -2\tau_1 \\ -\tau_1 & 0 & k^2 + v_2 + \tau_2 \end{bmatrix}, \tag{14}
$$

where the parameters τ_1, τ_2, v_2 are defined [26] through the expansions of the gauge kinetic function and scalar potential around the infrared value of the scalar ϕ_0,

$$
f = f_0 \left(1 + \tau_1(\phi - \phi_0) - \frac{\tau_2}{2}(\phi - \phi_0)^2 + \cdots \right), \tag{15}
$$

$$
V = v_0 \left(1 - \tau_1(\phi - \phi_0) - \frac{v_2}{2}(\phi - \phi_0)^2 + \cdots \right). \tag{16}
$$

Notice that $f_0 > 0$ and $v_0 < 0$ and the equations of motion (9)–(10) were used to relate to each other the terms linear in ϕ.

Spatially modulated instabilities in this system are present when, at finite momentum, at least one of the mass eigenvalues violates the AdS$_2$ BF bound, i.e. when $m_i^2 < -\frac{1}{4}$. Here we are going to focus exclusively on the static, $\omega = 0$ modes appearing at the onset of the instability. From the structure of the mass matrix, we immediately see that the eigenvalues m_i^2 are controlled by τ_1 and the combination $(\tau_2 + v_2)$. Finally, the fact that these instabilities are triggered without the need for P or T violation is reflected by the structure of the mass matrix, which depends only on k^2 and not on k. It is also reflected by the fact that the "dangerous" modes are indeed static and correspond to $\delta g_{tx_1} = \delta A_{x_1} = 0$ [26].

A. Conditions for instabilities

In the zero momentum case, the mass matrix simplifies and one finds

$$
m_i^2 = \{0, 2, 2\tau_1^2 + \tau_2 + v_2\}. \tag{17}
$$

Thus, the system will have unstable modes already at $k = 0$ when the parameters are such that

$$
2\tau_1^2 + \tau_2 + v_2 < -\frac{1}{4}. \tag{18}
$$

However, these perturbations do not break translation invariance and should indicate instabilities to the formation of other AdS$_2 \times \mathbb{R}^2$ solutions or geometries conformal to it. Since here we are interested in (stripe) instabilities triggered at finite momentum, we will work under the assumption that (18) is never satisfied, so that all the eigenvalues (17) are guaranteed to be above the AdS$_2$ BF bound.

At finite momentum the eigenvalues can be solved for exactly, but are significantly cumbersome. We start by working in a small momentum approximation, which will be enough to illustrate the main point we are after. For a

---

[2]The perturbations are left invariant by a coordinate transformation combined with a $U(1)$ gauge transformation, discussed in detail in [26].

[3]We are using the mass matrix notation of [26].

couple of special parameter choices, we will also make use of the exact eigenvalues.

Small momentum expansion. Assuming that the matrix eigenvalues have a momentum expansion of the form

$$\lambda = \lambda_0 + k^2 \lambda_1 + \mathcal{O}(k^4),$$

and using the fact that we know their zero-momentum values λ_0 from (17), we find (provided that $\tau_2 + v_2 \neq -2\tau_1^2$) the following expressions:

$$m_1^2 = 0 + \mathcal{O}(k^4), \tag{19}$$

$$m_2^2 = 2 + k^2 \left(\frac{2\tau_1^2 + 2(\tau_2 + v_2) - 4}{2\tau_1^2 + (\tau_2 + v_2) - 2} \right) + \mathcal{O}(k^4), \tag{20}$$

$$m_3^2 = 2\tau_1^2 + (\tau_2 + v_2) + k^2 \left(\frac{4\tau_1^2 + (\tau_2 + v_2) - 2}{2\tau_1^2 + (\tau_2 + v_2) - 2} \right) + \mathcal{O}(k^4). \tag{21}$$

We will come back to the case $\tau_2 + v_2 = -2\tau_1^2$, which needs to be analyzed separately, shortly. Notice that to see potential instabilities associated with the first eigenvalue becoming negative we must go to higher order in momentum,

$$m_1^2 = \frac{1}{2} \left(\frac{\tau_2 + v_2}{2\tau_1^2 + \tau_2 + v_2} \right) k^4$$
$$+ \left(\frac{2\tau_1^2 - (\tau_2 + v_2)\tau_1^2 - (\tau_2 + v_2)^2}{2(2\tau_1^2 + \tau_2 + v_2)^2} \right) k^6 + \cdots.$$

Here we will content ourselves with examining the structure of the remaining two eigenvalues, neglecting terms of order $\mathcal{O}(k^4)$ and higher. We don't expect any qualitative differences by including higher order terms in momentum.

We will take the onset of the instability to be signaled by the condition that the k^2 dependent terms become negative—the logic being that for an appropriate value of the momentum $k = k_*$, this contribution will win over the leading $k = 0$ term, pushing at least one of the mass eigenvalues below the AdS$_2$ BF bound.[4] In particular, examining both m_2 and m_3, we see that the k-dependent terms become negative when

$$\boxed{1 - \frac{1}{2}(\tau_2 + v_2) < \tau_1^2 < 2 - (\tau_2 + v_2)}, \tag{22}$$

which we therefore identify with the "window" for instabilities (provided that $\tau_2 + v_2 \neq -2\tau_1^2$). Note that from this

---

[4]Clearly, this has to be done within the regime of validity of the small k eigenvalue approximation we are employing.

relation we learn that (small k) unstable modes are only possible for $\tau_2 + v_2 < 2$.

Exact eigenvalues. For certain parameter choices the mass eigenvalues are easy to analyze exactly, without resorting to any small momentum expansion:

(i) Case 1. The case $\tau_2 + v_2 = -2\tau_1^2$, which was omitted from the small k analysis above, gives

$$m_i^2 = \left\{ k^2, 1 + k^2 \pm \sqrt{1 + 2k^2(1 + \tau_1^2)} \right\}. \tag{23}$$

The last eigenvalue is the only one which can dip below the AdS$_2$ BF bound; in fact, it attains its lowest value at $k_*^2 = \frac{\tau_1^2(2 + \tau_1^2)}{2(1 + \tau_1^2)}$, where it equals

$$m_{min}^2 = -\frac{1}{2} \frac{\tau_1^4}{1 + \tau_1^2}. \tag{24}$$

Violations of the AdS$_2$ BF bound and therefore instabilities will occur whenever $m_{min}^2 < -\frac{1}{4}$, which translates to

$$\boxed{\tau_1^2 > 1.} \tag{25}$$

(ii) Case 2. Another special parameter choice is $\tau_2 + v_2 = 2$, which as we noted above "closes" the instability window (22). In this case, the mass matrix simplifies significantly and we have

$$m_1^2 = k^2 + 2,$$
$$m_{2,3}^2 = 1 + k^2 + \tau_1^2$$
$$+ \pm \sqrt{1 + 2k^2(1 + \tau_1^2) + 2\tau_1^2 + \tau_1^4}.$$

All the squared-mass eigenvalues are now non-negative (the third one attains its minimum at $k = 0$) and therefore we don't see any unstable modes, as anticipated from (22).

A more exhaustive analysis of the exact mass eigenvalues is beyond the scope of this paper.

IV. THE INTERMEDIATE SCALING REGIME

So far we have restricted our attention to the instabilities of AdS$_2 \times \mathbb{R}^2$ solutions to the class of models (1). However, what we are after is what they can teach us about the true ground state of the scaling solutions (3). Recall that our interest is in geometries which contain an intermediate $\{z, \theta\}$ scaling branch, and relax to AdS$_2 \times \mathbb{R}^2$ only in the deep IR. For solutions of this type, we can use the instability analysis of Sec. III to argue that the scaling geometries themselves should be thought of as being unstable—in the deep infrared—to spatially modulated phases. The relations (22) and (25) then translate into

conditions on the values of z and θ associated with infrared instabilities.

In order to introduce the 'minimal' set of ingredients needed to support the geometries (3), we assume a simple gauge kinetic function of the form

$$f(\phi) = e^{\alpha\phi}. \tag{26}$$

With this choice, the coefficients τ_1 and τ_2 defined in (15) are just

$$\tau_1 = \alpha, \qquad \tau_2 = -\alpha^2. \tag{27}$$

Next, we take the scalar potential to be of the form

$$V(\phi) = V_0 e^{-\eta\phi} + \mathcal{V}(\phi), \tag{28}$$

where we assume that the first term is responsible for driving the intermediate hyperscaling violating regime while $\mathcal{V}(\phi)$ is negligible there. Given these assumptions, the exponents z and θ can then be gotten from α and η by using (5). Finally, expanding the potential about ϕ_0, we extract

$$v_2 = L^2(\eta^2 V_0 e^{-\eta\phi_0} + \mathcal{V}'') = L^2(\mathcal{V}'' - \eta^2\mathcal{V}) - \eta^2, \tag{29}$$

where we made use of (9) and it is understood that $\mathcal{V}$ and $\mathcal{V}''$ are evaluated at ϕ_0.

Looking back at the small-momentum instability window (22) we derived in Sec. III, it can now be rewritten as

$$\alpha^2 > 2 - v_2 > 0, \tag{30}$$

or, entirely in terms of z, θ and $\mathcal{V}$:

$$\boxed{\begin{aligned}\frac{(\theta-4)^2}{(\theta-2)(\theta-2z+2)} &> 2 - L^2\mathcal{V}''(\phi_0) \\ + \frac{\theta^2}{(\theta-2)(\theta-2z+2)}&[1 + L^2\mathcal{V}(\phi_0)] > 0.\end{aligned}} \tag{31}$$

Scaling geometries with an infrared AdS_2 completion and whose $\{z, \theta\}$ exponents satisfy this inequality—for appropriate values of $\mathcal{V}(\phi_0)$ and $\mathcal{V}''(\phi_0)$—will then be unstable to the formation of spatially modulated phases. The NEC conditions (7) should also be imposed and further constrain the range of z and θ, as we show below. Although we won't do it here, imposing thermodynamical stability would lead to additional restrictions.

Perhaps more interesting is case 1, which had a simple exact solution and exhibited instabilities when (25) was satisfied. What this condition tells us is that scaling solutions with z and θ in the range

$$\boxed{\frac{(\theta-4)^2}{(\theta-2)(\theta-2z+2)} > 1} \tag{32}$$

will have spatially modulated fluctuations provided $\mathcal{V}(\phi)$ satisfies the following relation:

$$\frac{8}{\theta-2z+2} = L^2\left(\mathcal{V}''(\phi_0) - \frac{\theta^2}{(\theta-2)(\theta-2z+2)}\mathcal{V}(\phi_0)\right). \tag{33}$$

We illustrate case 1 in Fig. 1. The dark (blue) region contains the values of the exponents z and θ compatible with (32) and with the null energy conditions (7). Thus, it indicates the portion of phase space susceptible to instabilities for the analysis of case 1. The remaining light (pink) region represents values of $\{z, \theta\}$ allowed by NEC but outside of this particular instability window (see [29] for a plot of NEC for models with more complicated matter content). Note that for this case, the "special" value $\theta = 1$—associated with a log violation of the entanglement entropy in this number of dimensions—is associated with an unstable geometry for $1.5 \le z \le 6$.

In summary, for appropriate scalar potential profiles there will be regions of phase space in which conditions such as (31), (32) and (33) are easily satisfied. This suggests that—for the corresponding parameter choices—phases with spatial modulation are indeed the ultimate ground states of these classes of scaling solutions.
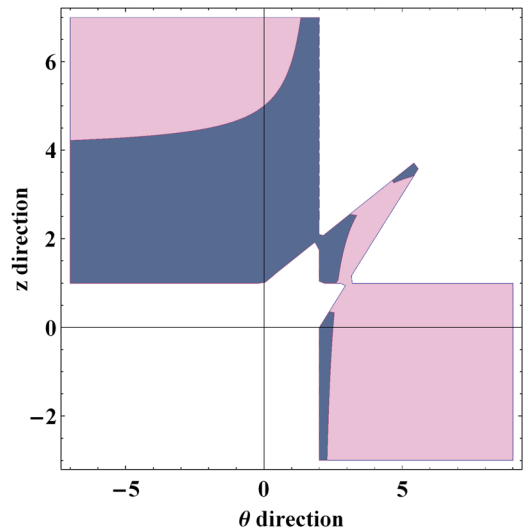
FIG. 1. The dark (blue) shaded region represents the values of z and θ compatible with NEC and associated with the spatially modulated instabilities predicted by (32) for case 1. The lighter (pink) shaded regions contains the remaining values of $\{z, \theta\}$ allowed by NEC but outside the instability window (32). We are plotting the range $-7 < \theta < 9$, $-3 < z < 7$.

A. Examples

For concreteness, we consider a few explicit examples:

(1) When $\mathcal{V}''(\phi_0) = \eta^2 \mathcal{V}(\phi_0)$, the expression (29) reduces to $v_2 = -\eta^2$. All the instabilities of the system then are controlled entirely by the values of α and η. This condition is clearly satisfied, for instance, when the full scalar potential is $V \sim \cosh \eta\phi$, a choice used in several constructions in the literature.

The small-k instability window (31) then takes the simple form

$$\alpha^2 - \eta^2 > 2. \tag{34}$$

Expressing it in terms of z and θ, we see that we should expect spatially modulated instabilities triggered by small momentum modes when

$$-4 < \theta - 2z + 2 < 0. \tag{35}$$

The NEC conditions further restrict the allowed range of z and θ, as shown in Fig. 2. As previously, the dark (blue) shaded region contains the values of z and θ compatible with NEC and susceptible to instabilities according to (35). The remaining lighter (pink) region represents the additional $\{z, \theta\}$ values allowed by NEC but which fall outside of this particular instability window.

In the Lorentz invariant case $z = 1$, the instability condition (35) becomes

$$-4 < \theta < 0, \tag{36}$$
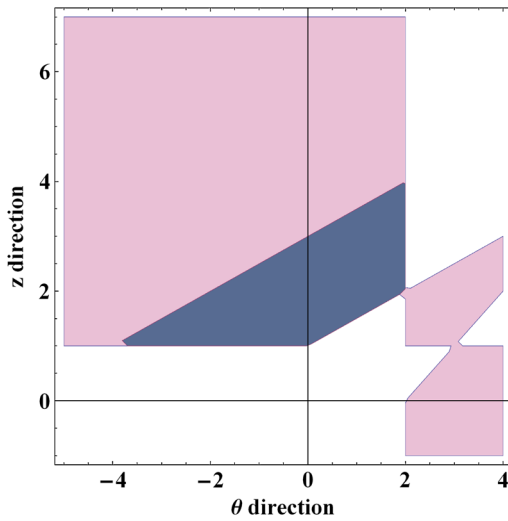
FIG. 2. The dark (blue) shaded region denotes the values of z and θ compatible with NEC and susceptible to instabilities, for the special example described by (35). The light (pink) region contains the remaining values of $\{z, \theta\}$ allowed by NEC.

while, when the hyperscaling violating exponent vanishes $\theta = 0$, it becomes

$$1 < z < 3. \tag{37}$$

Both conditions are automatically consistent with NEC. Finally, for the special $\theta = 1$ case, the instability window becomes

$$\frac{3}{2} < z < \frac{7}{2}, \tag{38}$$

also compatible with NEC. Notice that all of these relations are clearly visible in Fig. 2.

(2) For a racetrack-type potential,

$$V(\phi) = V_0 e^{-\eta\phi} + V_1 e^{\gamma\phi}, \tag{39}$$

requiring as usual an IR $AdS_2 \times \mathbb{R}^2$ and after some manipulations we find $v_2 = \alpha(\gamma - \eta) - \eta\gamma$. Small-$k$ perturbations then trigger instabilities when

$$0 < 2 + \alpha(\eta - \gamma) + \eta\gamma < \alpha^2, \tag{40}$$

or equivalently when

$$0 < 2 + \frac{\theta[4(1 - \kappa) + \theta(2\kappa - 1)]}{(\theta - 2)(\theta - 2z + 2)}$$
$$< \frac{(\theta - 4)^2}{(\theta - 2)(\theta - 2z + 2)}, \tag{41}$$

where we defined $\kappa \equiv \gamma/\eta$ for convenience.

On the other hand, the exact case 1 of Sec. III tells us that we should expect instabilities in the range (32) whenever $\gamma = -\alpha$. As usual, to satisfy NEC one must further impose (7).

(3) That these spatially modulated instabilities are quite generic, at least in the sense that models that exhibit them are easy to construct, should be by now clear. As one last example to further illustrate this point, consider

$$V(\phi) = V_0 e^{-\eta\phi} + V_1 e^{\gamma\phi} + V_2 e^{\delta\phi}. \tag{42}$$

Requiring $AdS_2 \times \mathbb{R}^2$ in the IR in this case gives

$$v_2 = -L^2 V_2 e^{\delta\phi_0}(\eta + \delta)(\gamma - \delta) + \alpha(\gamma - \eta) - \eta\gamma. \tag{43}$$

Looking for simplicity again at the instability window (32), recall that it will be valid provided that (33) is obeyed. For this potential, this boils down to choosing V_2 so that

$$V_2 = \frac{\alpha^2 + \alpha(\gamma - \eta) - \gamma\eta}{L^2 e^{\delta\phi_0}(\eta + \delta)(\gamma - \delta)}, \qquad (44)$$

a condition which should be easy to satisfy—apart from potential pathologies—irrespective of the values of the remaining Lagrangian parameters.

(4) Finally, we would like to point out that when the scalar potential is a single exponential,

$$V(\phi) = V_0 e^{-\eta\phi}, \qquad (45)$$

the requirement of $AdS_2 \times \mathbb{R}^2$ in the infrared forces $\alpha = \eta$. We then have

$$\tau_1 = \alpha, \qquad v_2 = \tau_2 = -\alpha^2, \qquad (46)$$

which "trivially" satisfies $\tau_2 + v_2 = -2\tau_1^2$ and is therefore an example of case 1. However, when $\alpha = \eta$ the solution corresponds to $z = \infty$ and is just $AdS_2 \times \mathbb{R}^2$ everywhere, with no intermediate regime of the type we have been describing.

V. FINAL REMARKS

For $\{z, \theta\}$ scaling solutions with an AdS_2 IR completion, the presence of finite-momentum modes which trigger instabilities in the near-horizon region can be used to argue that the full geometry should be expected to be unstable to spatially modulated phases. This logic led us to map the AdS_2 instability windows (22) and (25) we identified in Sec. III to conditions for the parameters z and θ characterizing the intermediate scaling regime—in a small-k approximation in (31) and for a simple exact case in (32). Depending on the detailed structure of the scalar potential, there will be regions of phase space in which such instability conditions are satisfied—in addition, models obeying these relations can be engineered in a straightforward manner.

A drawback of this analysis is that it doesn't allow one to make "universal" statements about which $\{z, \theta\}$ scaling solutions will be unstable, without fully specifying the scalar potential—knowledge of the infrared behavior of the geometry is clearly not enough to uniquely determine the intermediate scaling region. Moreover, while the perturbations we used here are more generic than those of [24], we have relied mostly on a small-k expansion, and therefore have not identified all possible sources of instability.

Nonetheless, the analysis in this paper reinforces the idea that spatially modulated phases seem to arise generically in the deep IR of a large class of scaling solutions with hyperscaling violation. While it would be interesting to have an explicit supergravity realization of the types of flows advocated here, there shouldn't be any fundamental obstacle to finding them. More broadly, it would be useful to have a better understanding of what differentiates between the possible IR completions of these classes of scaling solutions, and in particular whether they approach $AdS_2 \times \mathbb{R}^2$ or a geometry conformal to it, or even more general classes of anisotropic geometries—all cases associated with very different physics and transport properties. Further exploring the rich IR behavior of scaling solutions of this type—and properties of anisotropic and/or inhomogeneous ground states more generally—will undoubtedly continue to bring fresh insights into strongly correlated phases of matter.

[1] S. K. Domokos and J. A. Harvey, Baryon Number-Induced Chern-Simons Couplings of Vector and Axial-Vector Mesons in Holographic QCD, Phys. Rev. Lett. **99**, 141602 (2007).

[2] S. Nakamura, H. Ooguri, and C. -S. Park, Gravity dual of spatially modulated phase, Phys. Rev. D **81**, 044018 (2010).

[3] R. Flauger, E. Pajer, and S. Papanikolaou, A striped holographic superconductor, Phys. Rev. D **83**, 064009 (2011).

[4] A. Donos and J. P. Gauntlett, Holographic striped phases, J. High Energy Phys. 08 (2011) 140.

[5] N. Bao, S. Harrison, S. Kachru, and S. Sachdev, Vortex lattices and crystalline geometries, Phys. Rev. D **88**, 026002 (2013).

[6] M. Rozali, D. Smyth, E. Sorkin, and J. B. Stang, Holographic Stripes, Phys. Rev. Lett. **110**, 201603 (2013).

[7] A. Donos, Striped phases from holography, J. High Energy Phys. 05 (2013) 059.

[8] B. Withers, Black branes dual to striped phases, Classical Quantum Gravity **30**, 155025 (2013).

[9] B. Withers, The moduli space of striped black branes, arXiv:1304.2011.

[10] M. Rozali, D. Smyth, E. Sorkin, and J. B. Stang, Striped order in AdS/CFT, Phys. Rev. D **87**, 126007 (2013).

[11] S. S. Gubser and F. D. Rocha, Peculiar properties of a charged dilatonic black hole in AdS_5, Phys. Rev. D **81**, 046001 (2010).

[12] M. Cadoni, G. D'Appollonio, and P. Pani, Phase transitions between Reissner-Nordstrom and dilatonic black holes in 4D AdS spacetime, J. High Energy Phys. 03 (2010) 100.

[13] C. Charmousis, B. Gouteraux, B. S. Kim, E. Kiritsis, and R. Meyer, Effective holographic theories for low-temperature condensed matter systems, J. High Energy Phys. 11 (2010) 151.

[14] E. Perlmutter, Domain wall holography for finite temperature scaling solutions, J. High Energy Phys. 02 (2011) 013.

[15] N. Iizuka, N. Kundu, P. Narayan, and S. P. Trivedi, Holographic Fermi and non-Fermi liquids with transitions in dilaton gravity, J. High Energy Phys. 01 (2012) 094.

[16] B. Gouteraux and E. Kiritsis, Generalized holographic quantum criticality at finite density, J. High Energy Phys. 12 (2011) 036.

[17] L. Huijse, S. Sachdev, and B. Swingle, Hidden Fermi surfaces in compressible states of gauge-gravity duality, Phys. Rev. B **85**, 035121 (2012).

[18] S. Harrison, S. Kachru, and H. Wang, Resolving Lifshitz horizons, J. High Energy Phys. 02 (2014) 085.

[19] J. Bhattacharya, S. Cremonini, and A. Sinkovics, On the IR completion of geometries with hyperscaling violation, J. High Energy Phys. 02 (2013) 147.

[20] N. Kundu, P. Narayan, N. Sircar, and S. P. Trivedi, Entangled dilaton dyons, J. High Energy Phys. 03 (2013) 155.

[21] G. Knodel and J. T. Liu, Higher derivative corrections to Lifshitz backgrounds, J. High Energy Phys. 10 (2013) 002.

[22] A. Donos, J. P. Gauntlett, and C. Pantelidou, Magnetic and electric AdS solutions in string- and M-theory, Classical Quantum Gravity **29**, 194006 (2012).

[23] A. Donos, J. P. Gauntlett, and C. Pantelidou, Spatially modulated instabilities of magnetic black branes, J. High Energy Phys. 01 (2012) 061.

[24] S. Cremonini and A. Sinkovics, Spatially modulated instabilities of geometries with hyperscaling violation, J. High Energy Phys. 01 (2014) 099.

[25] N. Iizuka and K. Maeda, Stripe instabilities of geometries with hyperscaling violation, Phys. Rev. D **87**, 126006 (2013).

[26] A. Donos and J. P. Gauntlett, Holographic charge density waves, Phys. Rev. D **87**, 126008 (2013).

[27] N. Ogawa, T. Takayanagi, and T. Ugajin, Holographic Fermi surfaces and entanglement entropy, J. High Energy Phys. 01 (2012) 125.

[28] X. Dong, S. Harrison, S. Kachru, G. Torroba, and H. Wang, Aspects of holography for theories with hyperscaling violation, J. High Energy Phys. 06 (2012) 041.

[29] P. Bueno, W. Chemissany, and C. S. Shahbazi, On $hvLif$-like solutions in gauged supergravity, Eur. Phys. J. C **74**, 2684 (2014).